RMetS
Royal Meteorological Society

Adjoint sensitivity of the model forecast to data assimilation system error covariance parameters

Dacian N. Daescu[a]* and Ricardo Todling[b]†
[a]*Portland State University, Portland, Oregon, USA*
[b]*Global Modeling and Assimilation Office, NASA/GSFC, Greenbelt, Maryland, USA*
*Correspondence to: D. N. Daescu, Portland State University, PO Box 751, Portland, OR 97207, USA.
E-mail: daescu@pdx.edu
†The contribution of R. Todling to this article was prepared as part of his official duties as a US Federal Government employee.

The development of the adjoint of the forecast model and of the adjoint of the data assimilation system (adjoint-DAS) makes feasible the evaluation of the local sensitivity of a model forecast aspect with respect to a large number of parameters in the DAS. In this study it is shown that, by exploiting sensitivity properties that are intrinsic to the analyses derived from a minimization principle, the adjoint-DAS software tools developed at numerical weather prediction centres for observation and background sensitivity may be used to estimate the forecast sensitivity to observation- and background-error covariance parameters and for forecast impact assessment. All-at-once sensitivity to error covariance weighting coefficients and first-order impact estimates are derived as a particular case of the error covariance perturbation analysis. The use of the sensitivity information as a DAS diagnostic tool and for implementing gradient-based error covariance tuning algorithms is illustrated in idealized data assimilation experiments with the Lorenz 40-variable model. Preliminary results of forecast sensitivity to observation- and background-error covariance weight parameters are presented using the fifth-generation NASA Goddard Earth Observing System (GEOS-5) atmospheric DAS and its adjoint developed at the Global Modeling and Assimilation Office. **Copyright © 2010 Royal Meteorological Society**

Key Words: state analysis; parameter estimation; forecast impact; covariance tuning

Received 22 April 2010; Revised 28 July 2010; Accepted 3 August 2010; Published online in Wiley Online Library 11 October 2010

Citation: Daescu DN, Todling R. 2010. Adjoint sensitivity of the model forecast to data asimilation system error covariance parameters. *Q. J. R. Meteorol. Soc.* **136**: 2000–2012. DOI:10.1002/qj.693

1. Introduction

Atmospheric data assimilation techniques combine information from a model of the atmospheric dynamics, observational data, and error statistics to produce an analysis of the state of the atmosphere (Jazwinski, 1970; Daley, 1991; Kalnay, 2002). In practice, several simplifying assumptions are necessary to achieve a feasible implementation, and an increased amount of research in numerical weather prediction (NWP) is dedicated to observation- and background-error covariance modelling (Gaspari and Cohn, 1999; Hamill and Snyder, 2002; Lorenc, 2003; Buehner *et al.*, 2005; Frehlich, 2006; Janjić and Cohn, 2006; Bannister, 2008a,b) and to the development of effective techniques for diagnosis, estimation, and tuning of unknown error covariance parameters in both variational and Kalman filter-based assimilation systems (Dee, 1995; Dee and Da Silva, 1999; Desroziers and Ivanov, 2001; Desroziers *et al.*, 2005; Chapnik *et al.*, 2006; Desroziers *et al.*, 2009; Li *et al.*, 2009).

Valuable insight on the relative importance and contribution of the data assimilation system (DAS) components to reduce the forecast uncertainties may be

Copyright © 2010 Royal Meteorological Society

obtained by performing sensitivity studies to provide an assessment of the forecast impact as a result of variations in the DAS input. The development of the adjoint of the forecast model and of the adjoint of the data assimilation system (adjoint-DAS) makes feasible the evaluation of the derivative-based, local sensitivity (Cacuci, 2003) of a scalar forecast aspect with respect to a large number of DAS input components. Adjoint-DAS estimation of the observation sensitivity was considered in the work of Baker and Daley (2000) and Doerenbecher and Bergot (2001) as a tool to design observation targeting strategies. Subsequently, Langland and Baker (2004) have shown that the combined information derived from the adjoint of the forecast model and the adjoint-DAS may be used to provide a detailed (*all-at-once*) assessment of the observation impact on reducing the forecast errors in variational data assimilation (VDA). Adjoint-DAS tools have been developed at major NWP centres and are currently used to monitor the impact of data provided by the global observing network in reducing short-range forecasts errors, to provide data quality diagnostics and guidance for optimal satellite channel selection, and to design observation targeting strategies (Bergot and Doerenbecher, 2002; Fourrié *et al.*, 2002; Langland, 2005; Zhu and Gelaro, 2008; Baker and Langland, 2009; Cardinali, 2009; Gelaro and Zhu, 2009). A significant software development effort is required to implement the adjoint-DAS methodology, however this approach provides a detailed assessment of the contribution of each observing system component to the forecast error reduction that would be difficult to obtain by other means in VDA. Techniques for evaluating sensitivity to observations and observation impact assessment in an ensemble Kalman filter are discussed by Liu and Kalnay (2008) and Torn and Hakim (2008).

Proper weighting between the information content of the prior state estimate and of the observational data is necessary to optimize the DAS performance. To date, studies on the forecast impact as a result of variations in the observation-error variances have been performed only through additional assimilation experiments (Joiner *et al.*, 2007) and, given the multitude of data types, the increased computational cost prevents a comprehensive observing system analysis. The identification of those DAS components whose improvement in the estimates of the error statistics would be of most benefit to the analyses and forecasts is necessary for implementing efficient iterative procedures for tuning error covariance parameters. The study of Desroziers *et al.* (2009) shows that the impact of tuning observation- and background-error covariances using *a posteriori* diagnostics is closely determined by the specification of the short-range forecast score. Guidance to error covariance tuning algorithms and assessment of their potential impact on a specific forecast aspect may be obtained by evaluating the forecast sensitivity to the tuning parameters.

Le Dimet *et al.* (1997) provided the theoretical framework to sensitivity analysis in VDA. The derivation of the sensitivity equations and applications of the adjoint-DAS approach to error covariance sensitivity analysis in VDA are presented by Daescu (2008). The current work investigates novel adjoint-DAS applications to parametric error covariance sensitivity and forecast impact assessment and as a tool to provide DAS diagnostics. Section 2 includes a review of the forecast sensitivity to DAS input for analyses derived from a minimization principle. The rank-one matrix structure of the forecast sensitivity to the error covariances is emphasized and various sensitivity identities are established. In section 3, it is shown that error covariance sensitivity properties and the adjoint-DAS software tools developed at operational NWP centres for observation and background sensitivity may be used to estimate the forecast sensitivity to error covariance parameters and to provide a first-order impact assessment. The forecast sensitivity to error covariance weighting coefficients is derived as a particular case of the error covariance perturbation analysis. DAS optimality and sensitivity-based diagnostics are discussed in the context of linear estimation theory and a feasible approach to parameter tuning is presented. In section 4, idealized experiments are performed with the Lorenz 40-variable model to illustrate the potential use of the sensitivity information as a DAS diagnostic tool and to perform iterative error covariance tuning. Preliminary results of forecast sensitivity to observation- and background-error covariance weighting are presented using the fifth-generation NASA Goddard Earth Observing System (GEOS-5) atmospheric DAS and its adjoint. A summary and further research directions are in section 5.

2. Sensitivity analysis in VDA

Variational data assimilation (VDA) provides an analysis $\mathbf{x}^{\mathrm{a}} \in \mathbb{R}^n$ to the true state $\mathbf{x}^{\mathrm{t}}$ of the atmosphere by minimizing the cost functional

$$\begin{aligned} J(\mathbf{x}) &= J^{\mathrm{b}} + J^{\mathrm{o}} \\ &= \frac{1}{2}(\mathbf{x}-\mathbf{x}^{\mathrm{b}})^{\mathrm{T}}\mathbf{B}^{-1}(\mathbf{x}-\mathbf{x}^{\mathrm{b}}) \\ &+ \frac{1}{2}\left[\mathbf{h}(\mathbf{x})-\mathbf{y}\right]^{\mathrm{T}}\mathbf{R}^{-1}\left[\mathbf{h}(\mathbf{x})-\mathbf{y}\right], \qquad (1) \\ \mathbf{x}^{\mathrm{a}} &= \mathrm{Arg\ min}\, J, \qquad (2) \end{aligned}$$

where $\mathbf{x}^{\mathrm{b}} \in \mathbb{R}^n$ is a prior (background) state estimate, $\mathbf{y} \in \mathbb{R}^p$ is the vector of observational data, and $\mathbf{h}$ is the observation operator that maps the state into observations. In practice, statistical information on the background error $\boldsymbol{\epsilon}^{\mathrm{b}} = \mathbf{x}^{\mathrm{b}} - \mathbf{x}^{\mathrm{t}}$ and observational error $\boldsymbol{\epsilon}^{\mathrm{o}} = \mathbf{y} - \mathbf{h}(\mathbf{x}^{\mathrm{t}})$ is used to specify the weighting matrices $\mathbf{B} \in \mathbb{R}^{n\times n}$ and $\mathbf{R} \in \mathbb{R}^{p\times p}$ that are representations in the DAS of the background- and observation-error covariances $\mathbf{B}_{\mathrm{t}} = E(\boldsymbol{\epsilon}^{\mathrm{b}}\boldsymbol{\epsilon}^{\mathrm{b}\mathrm{T}})$ and $\mathbf{R}_{\mathrm{t}} = E(\boldsymbol{\epsilon}^{\mathrm{o}}\boldsymbol{\epsilon}^{\mathrm{o}\mathrm{T}})$ respectively, where $E(\cdot)$ denotes the statistical expectation operator. If the observation operator is assumed to be linear, $\mathbf{h}(\mathbf{x}) = \mathbf{H}\mathbf{x}$, the analysis (2) is expressed as

$$\mathbf{x}^{\mathrm{a}} = \mathbf{x}^{\mathrm{b}} + \mathbf{K}[\mathbf{y} - \mathbf{H}\mathbf{x}^{\mathrm{b}}], \qquad (3)$$

where the gain matrix $\mathbf{K}$ is defined as

$$\begin{aligned} \mathbf{K} &= \left[\mathbf{B}^{-1} + \mathbf{H}^{\mathrm{T}}\mathbf{R}^{-1}\mathbf{H}\right]^{-1}\mathbf{H}^{\mathrm{T}}\mathbf{R}^{-1} \\ &= \mathbf{B}\mathbf{H}^{\mathrm{T}}\left[\mathbf{H}\mathbf{B}\mathbf{H}^{\mathrm{T}} + \mathbf{R}\right]^{-1}. \qquad (4) \end{aligned}$$

In four-dimensional variational data assimilation (4D-Var) the operator $\mathbf{h}$ incorporates the nonlinear model to properly account for time-distributed data and an outer-loop iteration (Courtier *et al.*, 1994; Rosmond and Xu, 2006; Trémolet, 2007a) is used to approximate the solution to the nonlinear problem (1)–(2).

Copyright © 2010 Royal Meteorological Society

2.1. Observation and background sensitivity

Baker and Daley (2000) derived the equations of the sensitivity (gradient) of a scalar forecast aspect $e(\mathbf{x}^{\mathrm{a}})$ to observations and background for a linear analysis scheme (3)–(4):

$$\nabla_{\mathbf{y}} e(\mathbf{x}^{\mathrm{a}}) = \mathbf{K}^{\mathrm{T}} \nabla_{\mathbf{x}} e(\mathbf{x}^{\mathrm{a}}), \quad (5)$$

$$\nabla_{\mathbf{x}^{\mathrm{b}}} e(\mathbf{x}^{\mathrm{a}}) = [\mathbf{I} - \mathbf{H}^{\mathrm{T}}\mathbf{K}^{\mathrm{T}}] \nabla_{\mathbf{x}} e(\mathbf{x}^{\mathrm{a}}). \quad (6)$$

Typically, the forecast score is defined as a short-range forecast error measure

$$e(\mathbf{x}^{\mathrm{a}}) = (\mathbf{x}_{\mathrm{f}}^{\mathrm{a}} - \mathbf{x}_{\mathrm{f}}^{\mathrm{v}})^{\mathrm{T}} \mathbf{C} (\mathbf{x}_{\mathrm{f}}^{\mathrm{a}} - \mathbf{x}_{\mathrm{f}}^{\mathrm{v}}), \quad (7)$$

where $\mathbf{x}_{\mathrm{f}}^{\mathrm{a}} = M_{t_0 \to t_{\mathrm{f}}}(\mathbf{x}^{\mathrm{a}})$ is the nonlinear model forecast at verification time t_{f}, $\mathbf{x}_{\mathrm{f}}^{\mathrm{v}}$ is the verifying analysis at t_{f} and serves as a proxy to the true state $\mathbf{x}_{\mathrm{f}}^{\mathrm{t}}$, and $\mathbf{C}$ is an appropriate symmetric and positive semidefinite matrix that defines the metric in the state space, e.g. the total energy norm, and may incorporate a regional projection operator. Evaluation of the sensitivities (5) and (6) is performed by applying the *adjoint-DAS* operator $\mathbf{K}^{\mathrm{T}}$ to the vector $\nabla_{\mathbf{x}} e(\mathbf{x}^{\mathrm{a}})$ of forecast sensitivity to analysis. The latter is obtained by integrating the adjoint $\mathbf{M}^{\mathrm{T}}$ of the tangent linear model along the trajectory initiated from $\mathbf{x}^{\mathrm{a}}$:

$$\nabla_{\mathbf{x}} e(\mathbf{x}^{\mathrm{a}}) = 2[\mathbf{M}_{t_0 \to t_{\mathrm{f}}}(\mathbf{x}^{\mathrm{a}})]^{\mathrm{T}} \mathbf{C} (\mathbf{x}_{\mathrm{f}}^{\mathrm{a}} - \mathbf{x}_{\mathrm{f}}^{\mathrm{v}}). \quad (8)$$

Additional simplifying assumptions are necessary to alleviate the need for higher-order derivative information in the sensitivity computations when multiple outer-loop iterations are used to obtain an approximation to the solution to (1), as discussed by Trémolet (2008).

2.2. Adjoint-DAS observation impact estimation

The adjoint-DAS approach to observation impact (OBSI) estimation relies on the observation-space evaluation of the change in the forecast due to assimilation of all data in the DAS,

$$\delta e = e(\mathbf{x}^{\mathrm{a}}) - e(\mathbf{x}^{\mathrm{b}}) \approx (\delta \mathbf{y})^{\mathrm{T}} \mathbf{g}, \quad (9)$$

in terms of the innovation vector $\delta \mathbf{y} = \mathbf{y} - \mathbf{h}(\mathbf{x}^{\mathrm{b}})$ and a properly defined weight vector $\mathbf{g}$ that is expressed in terms of the adjoint-DAS operator $\mathbf{K}^{\mathrm{T}}$ and the forecast sensitivity to initial conditions (Gelaro *et al.*, 2007). A measure of the contribution of individual data components to forecast-error reduction, per observation type, instrument type, and data location, is obtained by taking the inner product between the innovation vector component and the corresponding $\delta \mathbf{y}$-amplification factor in (9):

$$I(\mathbf{y}_i) = (\delta \mathbf{y}_i)^{\mathrm{T}} \mathbf{g}_i, \quad (10)$$

where $\mathbf{y}_i$ is the data subset whose impact is being evaluated. Data components with $I(\mathbf{y}_i) < 0$ contribute to the forecast-error reduction (improve the forecast), whereas data components with $I(\mathbf{y}_i) > 0$ will increase the forecast error (degrade the forecast). The second-order accurate δe-approximation measure,

$$\delta e \approx (\delta \mathbf{y})^{\mathrm{T}} \mathbf{K}^{\mathrm{T}} \left[\frac{1}{2} \nabla_{\mathbf{x}} e(\mathbf{x}^{\mathrm{b}}) + \frac{1}{2} \nabla_{\mathbf{x}} e(\mathbf{x}^{\mathrm{a}}) \right], \quad (11)$$

has been first considered in the work of Langland and Baker (2004) and in recent adjoint-based OBSI studies (Cardinali, 2009; Gelaro and Zhu, 2009). Efficient alternatives to (11), such as a midpoint rule, are discussed by Daescu and Todling (2009).

2.3. Error covariance sensitivity

Implicit differentiation applied to the first-order optimality condition $\nabla_{\mathbf{x}} J(\mathbf{x}^{\mathrm{a}}) = \mathbf{0}$ to (1)

$$\mathbf{B}^{-1}(\mathbf{x}^{\mathrm{a}} - \mathbf{x}^{\mathrm{b}}) + \mathbf{H}^{\mathrm{T}} \mathbf{R}^{-1} [\mathbf{h}(\mathbf{x}^{\mathrm{a}}) - \mathbf{y}] = \mathbf{0}, \quad (12)$$

where $\mathbf{H} = \partial \mathbf{h} / \partial \mathbf{x} \in \mathbb{R}^{p \times n}$ is the Jacobian matrix of the observation operator at $\mathbf{x}^{\mathrm{a}}$, allows close relationships to be established between the forecast sensitivities to observations/background and to the associated error covariances (Daescu, 2008):

$$\nabla_{\mathbf{y}} e(\mathbf{x}^{\mathrm{a}}) = \mathbf{R}^{-1} \mathbf{H} \mathbf{A} \nabla_{\mathbf{x}} e(\mathbf{x}^{\mathrm{a}}), \quad (13)$$

$$\frac{\partial e(\mathbf{x}^{\mathrm{a}})}{\partial \mathbf{R}} = \nabla_{\mathbf{y}} e(\mathbf{x}^{\mathrm{a}}) \left[\mathbf{h}(\mathbf{x}^{\mathrm{a}}) - \mathbf{y} \right]^{\mathrm{T}} \mathbf{R}^{-1}, \quad (14)$$

$$\nabla_{\mathbf{x}^{\mathrm{b}}} e(\mathbf{x}^{\mathrm{a}}) = \mathbf{B}^{-1} \mathbf{A} \nabla_{\mathbf{x}} e(\mathbf{x}^{\mathrm{a}}), \quad (15)$$

$$\frac{\partial e(\mathbf{x}^{\mathrm{a}})}{\partial \mathbf{B}} = \nabla_{\mathbf{x}^{\mathrm{b}}} e(\mathbf{x}^{\mathrm{a}}) \left[\mathbf{x}^{\mathrm{a}} - \mathbf{x}^{\mathrm{b}} \right]^{\mathrm{T}} \mathbf{B}^{-1}, \quad (16)$$

where

$$\mathbf{A} = \left[\nabla_{\mathbf{xx}}^2 J(\mathbf{x}^{\mathrm{a}}) \right]^{-1} \quad (17)$$

denotes the inverse of the Hessian matrix of the cost (1) at $\mathbf{x}^{\mathrm{a}}$ and it is assumed to be a positive definite matrix. In particular, for a linear observational operator the inverse Hessian is the state independent matrix

$$\mathbf{A} = \left[\mathbf{B}^{-1} + \mathbf{H}^{\mathrm{T}} \mathbf{R}^{-1} \mathbf{H} \right]^{-1}. \quad (18)$$

If the observational errors are assumed to be uncorrelated, the error covariance matrix $\mathbf{R}$ is diagonal, $\mathbf{R} = \mathrm{diag}(\boldsymbol{\sigma}_{\mathrm{o}}^2)$, where $\boldsymbol{\sigma}_{\mathrm{o}}^2$ denotes the p-dimensional vector of observational-error variances. In this context, the forecast gradient to $\boldsymbol{\sigma}_{\mathrm{o}}^2$ may be expressed from (14) as

$$\nabla_{\boldsymbol{\sigma}_{\mathrm{o}}^2} e(\mathbf{x}^{\mathrm{a}}) = \left[\mathbf{R}^{-1} (\mathbf{h}(\mathbf{x}^{\mathrm{a}}) - \mathbf{y}) \right] \circ \nabla_{\mathbf{y}} e(\mathbf{x}^{\mathrm{a}}) \in \mathbb{R}^p, \quad (19)$$

where $\circ$ denotes the Hadamard (componentwise) product.

Equations (13) to (16) are derived directly from the optimality condition (12) and for a quadratic cost they are valid both in an observation space and in a state space DAS (4). In Daescu (2008), the error covariance sensitivity equations (14) and (16) were expressed in column vector format. The matrix format adopted here emphasizes the rank-one property of the **B**- and **R**-forecast sensitivity matrices, and it is more suitable for the purpose of this study. The equivalence between the two formulations is shown in the appendix.

By expressing the optimality condition (12) as

$$\mathbf{B}^{-1}(\mathbf{x}^{\mathrm{a}} - \mathbf{x}^{\mathrm{b}}) = \mathbf{H}^{\mathrm{T}} \mathbf{R}^{-1} [\mathbf{y} - \mathbf{h}(\mathbf{x}^{\mathrm{a}})] \quad (20)$$

and, after replacing (20) in (16), the forecast **B**-sensitivity may be equivalently expressed as

$$\frac{\partial e(\mathbf{x}^{\mathrm{a}})}{\partial \mathbf{B}} = \nabla_{\mathbf{x}^{\mathrm{b}}} e(\mathbf{x}^{\mathrm{a}}) [\mathbf{y} - \mathbf{h}(\mathbf{x}^{\mathrm{a}})]^{\mathrm{T}} \mathbf{R}^{-1} \mathbf{H}. \quad (21)$$

Copyright © 2010 Royal Meteorological Society

The following relationship between the observation sensitivity and the backgound sensitivity is an intrinsic property of the nonlinear VDA problem (1)–(2) and may be established from (12), (13), and (15):

$$\left[\mathbf{h}(\mathbf{x}^{\mathrm{a}})-\mathbf{y}\right]^{\mathrm{T}}\nabla_{\mathbf{y}}e(\mathbf{x}^{\mathrm{a}})+(\mathbf{x}^{\mathrm{a}}-\mathbf{x}^{\mathrm{b}})^{\mathrm{T}}\nabla_{\mathbf{x}^{\mathrm{b}}}e(\mathbf{x}^{\mathrm{a}})=0. \qquad (22)$$

The identity (22) is valid for any forecast aspect and its significance is further discussed in section 3.

3. Forecast impact and parametric error covariance sensitivity

While the explicit evaluation and storage of the error covariance sensitivity matrices is not feasible in an operational system, in particular for the **B**-sensitivity, from (14) and (16)/(21) it is noticed that evaluation and storage of only a few vectors are necessary to capture the information content of the error covariance sensitivities. Their use in an operator format may be considered, and of significant importance is the practical ability to provide *directional derivatives* associated with perturbations $(\delta\mathbf{B},\delta\mathbf{R})$ and sensitivities to key parameters used to model the error covariances. The mathematical formalism to exploit these adjoint-DAS capabilities and sensitivity applications are discussed in this section.

The forecast aspect $e(\mathbf{x}^{\mathrm{a}})$ is implicitly a function of the specification of the error covariances in the DAS, $e(\mathbf{B},\mathbf{R})=e[\mathbf{x}^{\mathrm{a}}(\mathbf{B},\mathbf{R})]$, and a first-order approximation to the forecast impact as a result of variations $\delta\mathbf{B}$ and $\delta\mathbf{R}$ in the specification of the error covariances may be expressed using the error covariance gradients

$$\begin{aligned}\delta e &= e(\mathbf{B}+\delta\mathbf{B},\mathbf{R}+\delta\mathbf{R})-e(\mathbf{B},\mathbf{R})\\ &\approx\left\langle\frac{\partial e}{\partial\mathbf{B}},\delta\mathbf{B}\right\rangle_{n\times n}+\left\langle\frac{\partial e}{\partial\mathbf{R}},\delta\mathbf{R}\right\rangle_{p\times p},\end{aligned} \qquad (23)$$

where

$$\langle\mathbf{X},\mathbf{Y}\rangle=\mathrm{Tr}\left(\mathbf{X}\mathbf{Y}^{\mathrm{T}}\right) \qquad (24)$$

denotes the Frobenius inner product on the vector space of matrices of the same order and is expressed in terms of the matrix trace operator Tr. The right side of (23) is the $(\delta\mathbf{B},\delta\mathbf{R})$-directional derivative of $e(\mathbf{B},\mathbf{R})$. The observation-error covariance matrix has a block diagonal structure associated with data subsets $\mathbf{y}_i\in\mathbb{R}^{p_i}, i\in I$, with uncorrelated observational errors

$$\mathbf{R}=\mathrm{diag}(\mathbf{R}_i),\quad \mathbf{R}_i\in\mathbb{R}^{p_i\times p_i},\quad i\in I. \qquad (25)$$

For practical purposes, each of the perturbations $\delta\mathbf{B}$ and $\delta\mathbf{R}_i$ are assumed to be symmetric matrices

$$\delta\mathbf{B}=(\delta\mathbf{B})^{\mathrm{T}},\quad \delta\mathbf{R}_i=(\delta\mathbf{R}_i)^{\mathrm{T}}, \qquad (26)$$

and are additionally constrained to preserve the positive definite property of $\mathbf{B}+\delta\mathbf{B}$, $\mathbf{R}+\delta\mathbf{R}$ as well as physical properties such as balance constraints (Bannister, 2008b). For example, such perturbations may arise in practice in the context of multiplicative/additive error covariance inflation techniques and as a result of variations in parameters used to model the error decorrelation length-scales.

The linear approximation (23) is the sum of the first-order impacts of individual error covariance perturbations $\delta\mathbf{B}$ and $\delta\mathbf{R}_i$:

$$\delta e\approx\mathrm{Tr}\left(\frac{\partial e}{\partial\mathbf{B}}\delta\mathbf{B}\right)+\sum_{i\in I}\mathrm{Tr}\left(\frac{\partial e}{\partial\mathbf{R}_i}\delta\mathbf{R}_i\right). \qquad (27)$$

Evaluation of the right-side terms in (27) is computationally feasible by properly exploiting the outer vector product structure of the error covariance sensitivities (16) and (14) and properties of the matrix trace operator. For example, evaluation of the first-order approximation to the impact δe_i associated with the observation-error covariance perturbation $\delta\mathbf{R}_i$ proceeds as follows:

$$\begin{aligned}\delta e_i &\approx \mathrm{Tr}\left(\frac{\partial e}{\partial\mathbf{R}_i}\delta\mathbf{R}_i\right)\\ &= \mathrm{Tr}\left(\nabla_{\mathbf{y}_i}e(\mathbf{x}^{\mathrm{a}})\left[\mathbf{h}_i(\mathbf{x}^{\mathrm{a}})-\mathbf{y}_i\right]^{\mathrm{T}}\mathbf{R}_i^{-1}\delta\mathbf{R}_i\right)\\ &= \mathrm{Tr}\left(\delta\mathbf{R}_i\nabla_{\mathbf{y}_i}e(\mathbf{x}^{\mathrm{a}})\left[\mathbf{h}_i(\mathbf{x}^{\mathrm{a}})-\mathbf{y}_i\right]^{\mathrm{T}}\mathbf{R}_i^{-1}\right)\\ &= \mathrm{Tr}\left\{\left[\delta\mathbf{R}_i\nabla_{\mathbf{y}_i}e(\mathbf{x}^{\mathrm{a}})\right]\left[\mathbf{R}_i^{-1}\{\mathbf{h}_i(\mathbf{x}^{\mathrm{a}})-\mathbf{y}_i\}\right]^{\mathrm{T}}\right\}.\end{aligned} \qquad (28)$$

The trace operator property $\mathrm{Tr}(\mathbf{a}\mathbf{b}^{\mathrm{T}})=\mathbf{b}^{\mathrm{T}}\mathbf{a}$ is valid for any column vectors of the same order and may be used to express (28) as

$$\delta e_i\approx\left[\mathbf{R}_i^{-1}(\mathbf{h}_i(\mathbf{x}^{\mathrm{a}})-\mathbf{y}_i)\right]^{\mathrm{T}}\left[\delta\mathbf{R}_i\nabla_{\mathbf{y}_i}e(\mathbf{x}^{\mathrm{a}})\right], \qquad (29)$$

which is the equation of the first-order approximation to the impact δe_i associated with the observation-error covariance perturbation $\delta\mathbf{R}_i$. In a similar fashion, the first-order approximation to the impact δe_{b} associated with the background-error covariance perturbation $\delta\mathbf{B}$ is expressed as

$$\delta e_{\mathrm{b}}\approx\left[\mathbf{B}^{-1}(\mathbf{x}^{\mathrm{a}}-\mathbf{x}^{\mathrm{b}})\right]^{\mathrm{T}}\left[\delta\mathbf{B}\nabla_{\mathbf{x}^{\mathrm{b}}}e(\mathbf{x}^{\mathrm{a}})\right]. \qquad (30)$$

From (29) and (30), it is noticed that, using the adjoint-DAS tools developed for observation and background sensitivity analysis, the evaluation of the linear approximation to the forecast impact δe_i and δe_{b} requires only the additional ability to provide the product between the error covariance perturbation matrix and the associated vector of forecast sensitivity to observations and to background, respectively.

Remark. It is noticed that, for any square matrices **X** and **Y** of the same order, if $\mathbf{Y}=\mathbf{Y}^{\mathrm{T}}$ then

$$\mathrm{Tr}\,(\mathbf{X}\mathbf{Y})=\mathrm{Tr}\left[\frac{1}{2}\left(\mathbf{X}+\mathbf{X}^{\mathrm{T}}\right)\mathbf{Y}\right], \qquad (31)$$

such that for any practical purposes the error covariance sensitivity matrices may be identified with their symmetric part

$$\left(\frac{\partial e}{\partial\mathbf{B}}\right)_s\ \stackrel{\mathrm{def}}{=}\ \frac{1}{2}\left[\left(\frac{\partial e}{\partial\mathbf{B}}\right)+\left(\frac{\partial e}{\partial\mathbf{B}}\right)^{\mathrm{T}}\right], \qquad (32)$$

$$\left(\frac{\partial e}{\partial\mathbf{R}}\right)_s\ \stackrel{\mathrm{def}}{=}\ \frac{1}{2}\left[\left(\frac{\partial e}{\partial\mathbf{R}}\right)+\left(\frac{\partial e}{\partial\mathbf{R}}\right)^{\mathrm{T}}\right]. \qquad (33)$$

Copyright © 2010 Royal Meteorological Society

3.1. Sensitivity to error covariance parameters

Forecast sensitivity to a scalar parameter s_i^o in the observation-error covariance representation $\mathbf{R}_i(s_i^o)$ is obtained by relating to a first order the error covariance variation $\delta\mathbf{R}_i$ to the parameter variation δs_i^o:

$$\delta\mathbf{R}_i \approx \frac{\partial \mathbf{R}_i(s_i^o)}{\partial s_i^o}\delta s_i^o. \tag{34}$$

From (29) and (34), the first-order approximation to the forecast impact is expressed as

$$\delta e_i \approx \left[\mathbf{R}_i^{-1}(s_i^o)(\mathbf{h}_i(\mathbf{x}^a)-\mathbf{y}_i)\right]^T\left[\frac{\partial \mathbf{R}_i(s_i^o)}{\partial s_i^o}\nabla_{\mathbf{y}_i}e(\mathbf{x}^a)\right]\delta s_i^o, \tag{35}$$

and the forecast sensitivity to the observation-error covariance parameter s_i^o is

$$\frac{\partial e(\mathbf{x}^a)}{\partial s_i^o} = \left[\mathbf{R}_i^{-1}(s_i^o)\{\mathbf{h}_i(\mathbf{x}^a)-\mathbf{y}_i\}\right]^T\left[\frac{\partial \mathbf{R}_i(s_i^o)}{\partial s_i^o}\nabla_{\mathbf{y}_i}e(\mathbf{x}^a)\right]. \tag{36}$$

In a similar fashion, the forecast sensitivity to a scalar parameter s^b in the background-error covariance representation $\mathbf{B}(s^b)$ is expressed as

$$\frac{\partial e(\mathbf{x}^a)}{\partial s^b} = \left[\mathbf{B}^{-1}(s^b)(\mathbf{x}^a-\mathbf{x}^b)\right]^T\left[\frac{\partial \mathbf{B}(s^b)}{\partial s^b}\nabla_{\mathbf{x}^b}e(\mathbf{x}^a)\right]. \tag{37}$$

For a practical implementation, the right-side terms of (36) and (37) may be computed without explicit evaluation of the derivative matrices $\partial\mathbf{R}_i/\partial s_i^o$ and $\partial\mathbf{B}/\partial s^b$ respectively, and the necessary matrix-vector products may be generated with the aid of automatic differentiation tools.

3.1.1. Sensitivity to multiplicative error covariance parameters

A particular case of practical significance is given by the parametric specification

$$\mathbf{B}(s^b) = s^b\mathbf{B}, \quad \mathbf{R}_i(s_i^o) = s_i^o\mathbf{R}_i, \quad i \in I, \tag{38}$$

which is a common representation used to perform error covariance tuning (Desroziers and Ivanov, 2001; Chapnik *et al.*, 2006; Desroziers *et al.*, 2009). Each of the error covariance parameters is a positive scalar, $s^b > 0, s_i^o > 0, i \in I$, and it is used to adjust the weight given in the analysis scheme to the background information and to the observation information, respectively. The parametric VDA cost functional associated with (38) is

$$J(\mathbf{s}) = \frac{1}{s^b}J^b + \sum_{i\in I}\frac{1}{s_i^o}J_i^o, \tag{39}$$

where $\mathbf{s}$ denotes the $(I+1)$-dimensional parameter vector of error covariance weights, $\mathbf{s} = [s^b, s_1^o, s_2^o, \ldots, s_I^o]$. The vector denoted $\overline{\mathbf{s}} = \mathbf{1}$ is obtained by setting all parameter values to 1 and corresponds to the error covariance specification $(\mathbf{B},\mathbf{R})$ in the DAS; the analysis associated with this DAS configuration is denoted $\overline{\mathbf{x}}^a = \mathbf{x}^a(\overline{\mathbf{s}})$. Variations δs^b and δs_i^o in the weighting coefficients are identified with variations in the specification of the error covariances:

$$\delta\mathbf{B} = \delta s^b\mathbf{B}, \tag{40}$$

$$\delta\mathbf{R}_i = \delta s_i^o\mathbf{R}_i, \quad i \in I. \tag{41}$$

Using a linearization in the parameter space at $\mathbf{s} = \overline{\mathbf{s}}$, the first-order estimate to the forecast impact δe as a result of weight variations $\delta\mathbf{s}$ is expressed as

$$\begin{aligned}\delta e &= e[\mathbf{x}^a(\overline{\mathbf{s}}+\delta\mathbf{s})] - e[\mathbf{x}^a(\overline{\mathbf{s}})]\\ &\approx \frac{\partial e(\overline{\mathbf{x}}^a)}{\partial s^b}\delta s^b + \sum_{i\in I}\frac{\partial e(\overline{\mathbf{x}}^a)}{\partial s_i^o}\delta s_i^o.\end{aligned} \tag{42}$$

From (36), (37) and (38), the forecast sensitivity to the background and observation weights at $\overline{\mathbf{s}} = \mathbf{1}$ is expressed respectively as

$$\frac{\partial e(\overline{\mathbf{x}}^a)}{\partial s^b} = \left[\overline{\mathbf{x}}^a - \mathbf{x}^b\right]^T\nabla_{\mathbf{x}^b}e(\overline{\mathbf{x}}^a), \tag{43}$$

$$\frac{\partial e(\overline{\mathbf{x}}^a)}{\partial s_i^o} = \left[\mathbf{h}_i(\overline{\mathbf{x}}^a) - \mathbf{y}_i\right]^T\nabla_{\mathbf{y}_i}e(\overline{\mathbf{x}}^a), \quad i \in I, \tag{44}$$

and

$$\begin{aligned}\delta e \approx\ & \delta s^b\left[\overline{\mathbf{x}}^a - \mathbf{x}^b\right]^T\nabla_{\mathbf{x}^b}e(\overline{\mathbf{x}}^a)\\ &+ \sum_{i\in I}\delta s_i^o\left[\mathbf{h}_i(\overline{\mathbf{x}}^a) - \mathbf{y}_i\right]^T\nabla_{\mathbf{y}_i}e(\overline{\mathbf{x}}^a)\end{aligned} \tag{45}$$

is the first-order approximation, in the parameter space, to the forecast impact of perturbations $\delta\mathbf{s}$ in the error covariance weights from the nominal value $\overline{\mathbf{s}} = \mathbf{1}$.

From (43) and (44), it is noticed that the identity (22) is equivalent to

$$\sum_{i\in I}\frac{\partial e(\overline{\mathbf{x}}^a)}{\partial s_i^o} + \frac{\partial e(\overline{\mathbf{x}}^a)}{\partial s^b} = 0 \tag{46}$$

and reflects an intrinsic property of the VDA optimization problem: multiplication of all error covariances in the DAS by the same (positive) constant has no impact on the analysis. For analysis impact purposes, the number of degrees of freedom in the parametric representation (39) is equal to I.

An observation space equation to the s^b-sensitivity is derived from (43) and (22)

$$\frac{\partial e(\overline{\mathbf{x}}^a)}{\partial s^b} = \left[\mathbf{y} - \mathbf{h}(\overline{\mathbf{x}}^a)\right]^T\nabla_{\mathbf{y}}e(\overline{\mathbf{x}}^a), \tag{47}$$

such that the information extracted from the analysis-minus-observed residuals and observation sensitivity provides *all-at-once* the sensitivities (44) and (47) to multiplicative error covariance weighting coefficients in the DAS configuration $(\mathbf{B},\mathbf{R})$, with negative s-derivative values indicating that, locally, the forecast error aspect is a decreasing function of the corresponding weight parameter. For example, a negative sensitivity (47) indicates that locally the forecast error aspect is a decreasing function of the s^b parameter and provides an indication that background-error covariance inflation is of potential benefit to the forecasts.

The sensitivity information may be used to provide *a priori* guidance to the forecast impact as a result of specified variations in individual weighting coefficients

$$\delta e_b \approx \frac{\partial e(\overline{\mathbf{x}}^a)}{\partial s^b}\delta s^b, \tag{48}$$

$$\delta e_i \approx \frac{\partial e(\overline{\mathbf{x}}^a)}{\partial s_i^o}\delta s_i^o. \tag{49}$$

Copyright © 2010 Royal Meteorological Society

A posteriori, the validity of the approximation (45) may be investigated for perturbations $\delta\mathbf{s}$ generated as the result of a tuning process, and (48) and (49) may be used to provide an assessment of the DAS components where tuning was of benefit ($\delta e_\mathrm{b} < 0$; $\delta e_i < 0$) or detrimental ($\delta e_\mathrm{b} > 0$; $\delta e_i > 0$) to the forecasts.

In VDA, the OBSI estimation using measures such as (11) and the evaluation of the sensitivities (44), (47) share the same adjoint-DAS tools and may be performed simultaneously using information from innovations $\mathbf{y} - \mathbf{h}(\mathbf{x}^\mathrm{b})$ and residuals $\mathbf{y} - \mathbf{h}(\mathbf{x}^\mathrm{a})$, respectively.

3.2. *DAS optimality and sensitivity diagnostics*

In the context of statistical linear estimation, information extracted from the innovations $\mathbf{y} - \mathbf{H}\mathbf{x}^\mathrm{b}$ and residuals $\mathbf{y} - \mathbf{H}\mathbf{x}^\mathrm{a}$ is used to derive consistency diagnostics of observation- and background-error statistics in the DAS (Talagrand, 1999; Daley and Barker, 2001; Desroziers *et al.*, 2005). Properties of the Best Linear Unbiased Estimator (BLUE) allow us to investigate the DAS optimality in terms of error covariance sensitivities in a linear analysis scheme (3)–(4). The analysis error $\boldsymbol{\epsilon}^\mathrm{a} = \mathbf{x}^\mathrm{a} - \mathbf{x}^\mathrm{t}$ is implicitly a function of the error covariance specification $(\mathbf{B}, \mathbf{R})$ in the DAS. Given a quadratic loss function

$$L(\boldsymbol{\epsilon}^\mathrm{a}) = \boldsymbol{\epsilon}^{\mathrm{a}\mathrm{T}}\mathbf{S}\boldsymbol{\epsilon}^\mathrm{a}, \tag{50}$$

where $\mathbf{S} \in \mathbb{R}^{n\times n}$ is a symmetric and positive semidefinite matrix, an optimal error covariance specification minimizes the expected loss (Jazwinski, 1970; Cohn, 1997) and a characteristic property of the BLUE is that the information-minus-analysis difference and the estimation error are statistically uncorrelated (Talagrand, 1999):

$$E[\boldsymbol{\epsilon}^\mathrm{a}(\mathbf{H}\mathbf{x}^\mathrm{a} - \mathbf{y})^\mathrm{T}] = \mathbf{0} \in \mathbb{R}^{n\times p}, \tag{51}$$

$$E[\boldsymbol{\epsilon}^\mathrm{a}(\mathbf{x}^\mathrm{a} - \mathbf{x}^\mathrm{b})^\mathrm{T}] = \mathbf{0} \in \mathbb{R}^{n\times n}. \tag{52}$$

By replacing

$$\nabla_{\mathbf{x}^\mathrm{a}} L = 2\mathbf{S}\,\boldsymbol{\epsilon}^\mathrm{a} \tag{53}$$

in the sensitivity equations (5), (6), (14) and (21), from (51) and (52) it is noticed that, in an optimal DAS, the expected value of the sensitivity to any of the entries in the background- and observation-error covariances is zero:

$$E\left(\frac{\partial L}{\partial \mathbf{B}}\right) = \mathbf{0} \in \mathbb{R}^{n\times n}, \quad E\left(\frac{\partial L}{\partial \mathbf{R}}\right) = \mathbf{0} \in \mathbb{R}^{p\times p}. \tag{54}$$

Simplifying assumptions are necessary to implement the error covariance sensitivity diagnostic (54) for parameter tuning and a major difficulty to overcome in practical applications is that analysis error estimates are not directly available in VDA. Valuable information may be obtained by collecting statistics of time series of data assimilation/forecast cycles (7) and analysis of the time-mean forecast sensitivity to error covariance parameters. The use of an ensemble of forecasts to define the functional aspect (7) provides a feasible approach for practical applications (Torn and Hakim, 2008).

The Kalman smoother theory to estimate the 4D-Var error statistics is discussed in the work of Ménard and Daley (1996). Iterative gradient-based algorithms for tuning a vector $\mathbf{s}$ of error covariance parameters may be implemented by solving the minimization problem

$$\min_{\mathbf{s}} e[\mathbf{x}^\mathrm{a}(\mathbf{s})]. \tag{55}$$

At each iteration

$$\mathbf{s}^{k+1} = \mathbf{s}^k + \alpha_k \mathbf{d}^k, \quad k = 0, 1, \ldots, \tag{56}$$

the analysis $\mathbf{x}^\mathrm{a}(\mathbf{s})$ is obtained as a solution to the VDA problem (1)–(2) and the adjoint-DAS approach provides the gradient information necessary to identify a descent direction $\mathbf{d}^k$ in the parameter space. The steepest descent direction

$$\mathbf{d}^k = -\nabla_{\mathbf{s}} e[\mathbf{x}^\mathrm{a}(\mathbf{s}^k)] \tag{57}$$

identifies the direction of small variations $\delta\mathbf{s}$, from the current DAS configuration, that will be of largest forecast benefit and provides a first-order error covariance diagnostic. In addition to the simplifying assumptions that are necessary to implement an iterative tuning algorithm, identifiability issues must be addressed in the estimation of error covariance parameters, as discussed by Dee and Da Silva (1999) and Chapnik *et al.* (2004).

4. Numerical experiments

The adjoint-DAS sensitivity approach as a DAS diagnostic tool and to perform error covariance parameter tuning is illustrated in idealized numerical experiments with the Lorenz-40 variable model (Lorenz and Emanuel, 1998)

$$\frac{\mathrm{d}x_j}{\mathrm{d}t} = (x_{j+1} - x_{j-2})\,x_{j-1} - x_j + F, \quad j = 1, 2, \ldots, n, \tag{58}$$

where $n = 40, x_{n+k} = x_k$, and $F = 8$. The system (58) is integrated with a fourth-order Runge–Kutta method and a constant time step $\Delta t = 0.05$ that in the data assimilation experiments is identified to a 6 h time period. The time evolution of the model state is expressed as

$$\mathbf{x}(t_{i+1}) = M_{t_i \to t_{i+1}}[\mathbf{x}(t_i)], \tag{59}$$

and the time evolution of the true state $\mathbf{x}^\mathrm{t}$ is obtained by adding at each time step a random state independent model error $\boldsymbol{\epsilon}^\mathrm{q}(t_i)$,

$$\mathbf{x}^\mathrm{t}(t_{i+1}) = M_{t_i \to t_{i+1}}[\mathbf{x}^\mathrm{t}(t_i)] + \boldsymbol{\epsilon}^\mathrm{q}(t_i) \tag{60}$$

which is taken from a normal distribution $N(0, \sigma_\mathrm{q}^2)$ and with the standard deviation specified as $\sigma_\mathrm{q} = 0.05$.

An initial state $\mathbf{x}_0^\mathrm{t}$ is obtained from a 90-day (360 time step) integration started from $x_j = 8$ for $j \neq n/2$ and $x_{n/2} = 8.008$; a background estimate $\mathbf{x}^\mathrm{b}$ to $\mathbf{x}_0^\mathrm{t}$ is prescribed by introducing random perturbations in $\mathbf{x}_0^\mathrm{t}$ taken from the standard normal distribution $N(0, 1)$. Observational data are generated from the true state $\mathbf{x}^\mathrm{t}$ at each time step and each grid point and it is assumed that the DAS incorporates two data types $\mathbf{y}^{(1)}$ and $\mathbf{y}^{(2)}$, each being a 20-dimensional vector, with uncorrelated observational errors. Data of type $\mathbf{y}^{(1)}$ are generated at odd locations $2j + 1, j = 0, 1, \ldots, 19$ with observation errors normally distributed, unbiased, and the standard deviation $\sigma_{\mathrm{o,t}}^{(1)} = 0.25$. Data of type $\mathbf{y}^{(2)}$

Copyright © 2010 Royal Meteorological Society

are generated at even locations $2j, j = 1, 2, \ldots, 20$ with observation errors normally distributed, unbiased, and the standard deviation $\sigma_{o,t}^{(2)} = 0.75$. Data of type $\mathbf{y}^{(1)}$ are thus of increased accuracy compared with data of type $\mathbf{y}^{(2)}$. In a first set of experiments (DAS-1), a *specification* of $\sigma_o^{(1)} = \sigma_o^{(2)} = 0.5$ is used in the DAS to investigate the ability of the adjoint-DAS approach to provide diagnosis and tuning of observation-error variances when deficiencies in the DAS are mainly due to mis-specified observational-error statistics. In DAS-1, at each observing site the errors in data $\mathbf{y}^{(1)}$ are overestimated, whereas the errors in data $\mathbf{y}^{(2)}$ are underestimated. DAS-1 implements a linear analysis scheme ((3)–(4)) and the background estimate at time t_{i+1} and the associated background-error covariance matrix are propagated using the Extended Kalman filter (EKF) equations

$$\mathbf{x}^{\mathrm{b}}(t_{i+1}) = M_{t_i \to t_{i+1}}(\mathbf{x}^{\mathrm{a}}(t_i)), \tag{61}$$

$$\mathbf{B}(t_{i+1}) = \mathbf{M}(t_i)\mathbf{A}(t_i)\mathbf{M}^{\mathrm{T}}(t_i) + \mathbf{Q}(t_i), \tag{62}$$

where $\mathbf{x}^{\mathrm{a}}(t_i)$ is the analysis (3) at time t_i,

$$\mathbf{A}(t_i) = \left[\mathbf{B}^{-1}(t_i) + \mathbf{H}^{\mathrm{T}}(t_i)\mathbf{R}^{-1}\mathbf{H}(t_i)\right]^{-1} = [\mathbf{I} - \mathbf{K}(t_i)\mathbf{H}(t_i)]\mathbf{B}(t_i) \tag{63}$$

is the inverse Hessian matrix associated to a quadratic cost (1), and $\mathbf{M}(t_i)$ is the state-dependent Jacobian matrix of the numerical model $M_{t_i \to t_{i+1}}$ from t_i to t_{i+1}. The model error covariance is prescribed as a time-invariant diagonal matrix $\mathbf{Q} = \mathrm{diag}(\boldsymbol{\sigma}_q^2)$.

DAS-1 is run for 3240 analysis cycles and a 24 h forecast error measure is collected over the last $N = 2880$ analysis cycles (a 2-year time period)

$$e[\mathbf{x}^{\mathrm{a}}(t_i)] = \left[\mathbf{x}_{\mathrm{f}}^{\mathrm{a}}(t_{i+4}) - \mathbf{x}^{\mathrm{v}}(t_{i+4})\right]^{\mathrm{T}}\left[\mathbf{x}_{\mathrm{f}}^{\mathrm{a}}(t_{i+4}) - \mathbf{x}^{\mathrm{v}}(t_{i+4})\right], \tag{64}$$

where $\mathbf{x}_{\mathrm{f}}^{\mathrm{a}}(t_{i+4}) = M_{t_i \to t_{i+4}}[\mathbf{x}^{\mathrm{a}}(t_i)]$ is the 24 h forecast state and $\mathbf{x}^{\mathrm{v}}(t_{i+4})$ is the verification state at t_{i+4}.

4.1. Observation impact estimation

Adjoint-DAS OBSI estimation is performed in DAS-1 using the approximation measure (11). Time-averaged OBSI estimates at each observing site are displayed in Figure 1(a) for a verification state specified as the true state, $\mathbf{x}^{\mathrm{v}}(t_{i+4}) = \mathbf{x}^{\mathrm{t}}(t_{i+4})$, and for a verification state produced by the DAS-1, $\mathbf{x}^{\mathrm{v}}(t_{i+4}) = \mathbf{x}^{\mathrm{a}}(t_{i+4})$, the latter being a typical choice in practical applications. The adjoint-DAS OBSI estimation properly identifies data of type $\mathbf{y}^{(1)}$ as data of increased forecast benefit compared with data of type $\mathbf{y}^{(2)}$. (Negative values indicate that assimilation of data contributes to the forecast error reduction.) It is noticed that the OBSI values based on a verification state produced by the DAS are overestimating the data impact on the actual forecast-error reduction and that underestimation of the observation-error variance in the DAS may result in a detrimental forecast impact, as seen for data of type $\mathbf{y}^{(2)}$ at observing site $j = 34$. The assessment of the state-to-observation space uncertainty propagation as a result of the errors in the verification state in deterministic OBSI estimation is an unresolved issue in NWP (Daescu, 2009).

4.2. Diagnosis of observation-error variances

The OBSI estimation provides valuable information on the contribution of individual datasets to the forecast-error reduction for a given specification of the error covariances in the DAS. Additional information is necessary to optimize the use of the observational data through proper specification of the error statistics and may be obtained from the observation-error covariance sensitivity analysis.

The time-averaged forecast sensitivity to the observation-error variance (19) at each observing site is displayed in Figure 1(b). It is noticed that at each observing site the first-order observation-error variance sensitivity diagnostic properly identifies data of type $\mathbf{y}^{(1)}$ as data where decreasing the error variance input in the DAS will reduce the forecast error (positive derivative values indicate that locally the functional aspect is an increasing function of the corresponding parameter). Data of type $\mathbf{y}^{(2)}$ are identified as data where increasing the error-variance input in the DAS will reduce the analysis/forecast error (negative derivative values indicate that locally the functional aspect is a decreasing function of the corresponding parameter). By analogy to the OBSI results, the sensitivity values are closely determined by the selection of the verification state and the specification $\mathbf{x}^{\mathrm{v}}(t_{i+4}) = \mathbf{x}^{\mathrm{a}}(t_{i+4})$ provided observation-error variance sensitivities of larger magnitude than $\mathbf{x}^{\mathrm{v}}(t_{i+4}) = \mathbf{x}^{\mathrm{t}}(t_{i+4})$.

4.3. Tuning of observation-error variances

The adjoint-DAS approach provides grounds for tuning the DAS observation-error variance input using a gradient-based iterative algorithm. The minimization functional is defined as a two-year time-averaged forecast-error measure (64)

$$e = \frac{1}{N}\sum_{i=1}^{N} e[\mathbf{x}^{\mathrm{a}}(t_i)], \tag{65}$$

and tuning is performed by solving the optimization problem

$$\min_{\boldsymbol{\sigma}_o^2} e\,. \tag{66}$$

This formulation involves a simplifying assumption in the evaluation of the gradient $\nabla_{\boldsymbol{\sigma}_o^2} e$, namely it neglects the time propagation of the $\delta\boldsymbol{\sigma}_o^2$ perturbation impact through various data assimilation cycles. Bound constraints $\boldsymbol{\sigma}_{o,\min}^2 \le \boldsymbol{\sigma}_o^2 \le \boldsymbol{\sigma}_{o,\max}^2$ are associated with (66) based on *a priori* estimates to min/max observation-error variances, and in the numerical experiments the observation-error standard deviation bounds are prescribed as $\boldsymbol{\sigma}_{o,\min} = 0.1$ and $\boldsymbol{\sigma}_{o,\max} = 1$. In particular, specification of an upper bound is necessary to avoid data denial (variances approaching infinity) in the tuning process when the verification state is produced by the DAS. The ability of the adjoint approach to accommodate an increased number of parameters is illustrated by performing tuning with the observation-error variance at each observing site as a free parameter (40-dimensional space). The evolution of the cost (65) during the minimization process is displayed in Figure 2(a) for a verification state produced by the DAS, $\mathbf{x}^{\mathrm{v}}(t_{i+4}) = \mathbf{x}^{\mathrm{a}}(t_{i+4})$, and for a verification

Copyright © 2010 Royal Meteorological Society

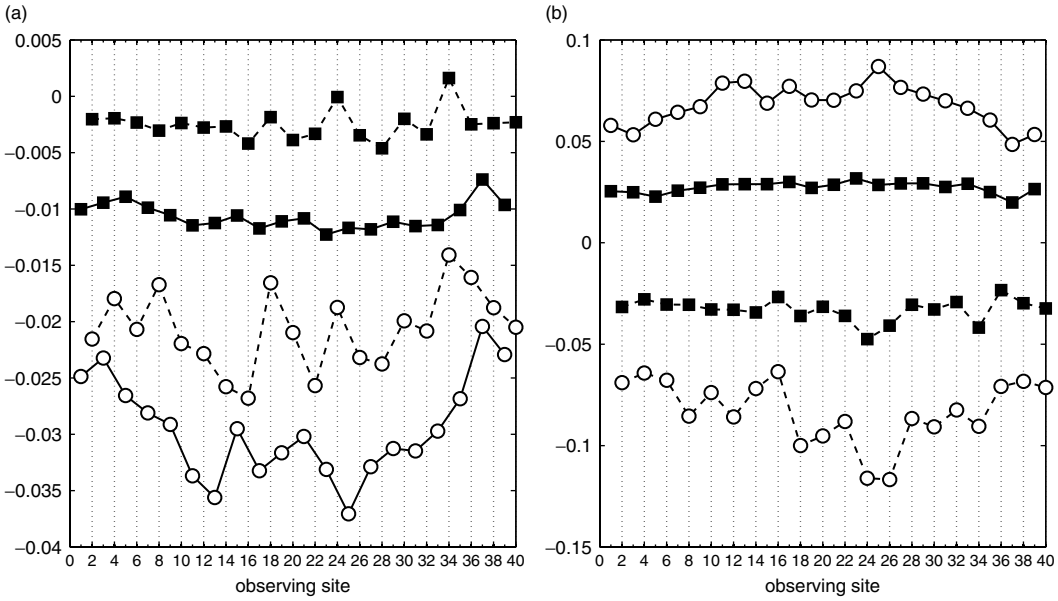

Figure 1. (a) Time-averaged observation impact estimation and (b) time-averaged sensitivity to observation-error variance in DAS-1. Results are from a verification state specified as the true state (squares) and with a verification state produced by the DAS-1 (circles). The solid and dashed lines correspond to observing sites of odd index and even index, respectively, and distinguish the two data types used in the DAS-1.

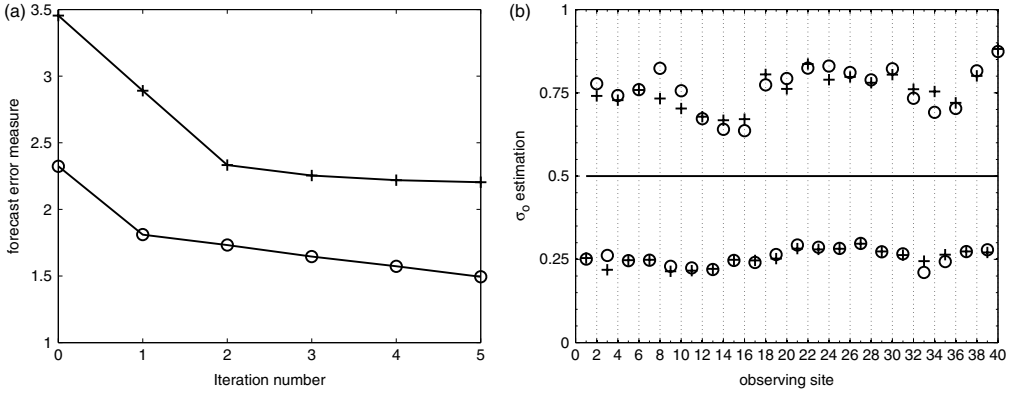

Figure 2. (a) Evolution of the forecast error aspect during the iterative tuning of observation-error variances, and (b) estimated observation-error standard deviation. The horizontal line in (b) indicates the initial specification of the observation-error standard deviation. Results are with a verification state specified as the true state (plus signs) and with a verification state produced by the DAS-1 (circles).

state prescribed as the true state, $\mathbf{x}^{\mathrm{v}}(t_{i+4}) = \mathbf{x}^{\mathrm{t}}(t_{i+4})$. The estimated observation-error standard deviation as a result of the tuning process is displayed in Figure 2(b). In both experiments, improved estimates were obtained within a few iterations, and it is noticed that the tuning process was able to properly distinguish between the underestimated and the overestimated observation-error variances. The results indicate an increased uncertainty propagation in the estimation of error variances associated with data of low forecast impact $\mathbf{y}^{(2)}$, compared with the estimation of error variances associated with data of high forecast impact $\mathbf{y}^{(1)}$.

4.4. *Diagnosis of mis-specified background-error correlations*

An additional set of experiments, DAS-2 and DAS-3, is used to illustrate the ability of the error covariance sensitivity information to provide diagnosis of mis-specified background-error correlations in the DAS. In both DAS-2 and DAS-3, the observation-error variances are set to be statistically consistent with the observational errors, $\sigma_{\mathrm{o}}^{(1)} = \sigma_{\mathrm{o,t}}^{(1)}$, $\sigma_{\mathrm{o}}^{(2)} = \sigma_{\mathrm{o,t}}^{(2)}$, and deficiencies are introduced in the DAS-3 through mis-specified background-error statistics. The DAS-2 is used as a reference system and provides an optimal analysis by evolving in time the background-error covariance according to the EKF equations. The time-averaged background-error covariance matrix over the 2-year analysis period in DAS-2 is displayed in Figure 3(a). The DAS-3 is a suboptimal system where the background-error covariance is prescribed as a diagonal matrix, frozen in time, with the diagonal entries fixed to their values at the beginning of the 2-year analysis period, as displayed in Figure 3(b). Background-error covariance sensitivity statistics are collected in DAS-3 for the 24-h forecast error measure (64) and in Figure 3(c) is shown the time-averaged forecast error **B**-sensitivity for a verification state prescribed as the true state. To extract the information relevant to symmetric perturbations, the results are displayed using the symmetric part (32). The **B**-sensitivity matrix in Figure 3(c) identifies the steepest descent direction in the background-error covariance space and, to a first order, provides guidance on the $\delta\mathbf{B}$ perturbation that is necessary to correct the background-error covariance in DAS-3 (Figure 3(b)) toward the optimal correlation structure in DAS-2 (Figure 3(a)).

Copyright © 2010 Royal Meteorological Society

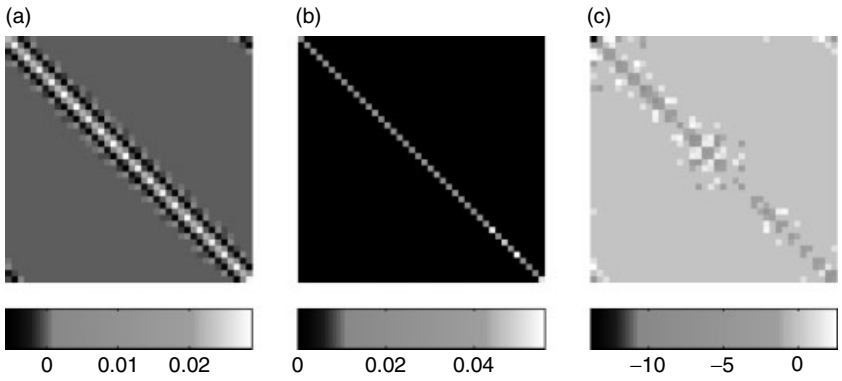

Figure 3. (a) Time-averaged background-error covariance matrix in DAS-2. (b) The background-error covariance in DAS-3 is specified as a time-invariant and diagonal matrix. (c) Time-averaged forecast-error sensitivity to the background-error covariance in DAS-3. The sensitivity matrix provides guidance on the perturbation structure that is necessary to correct (b) towards (a).

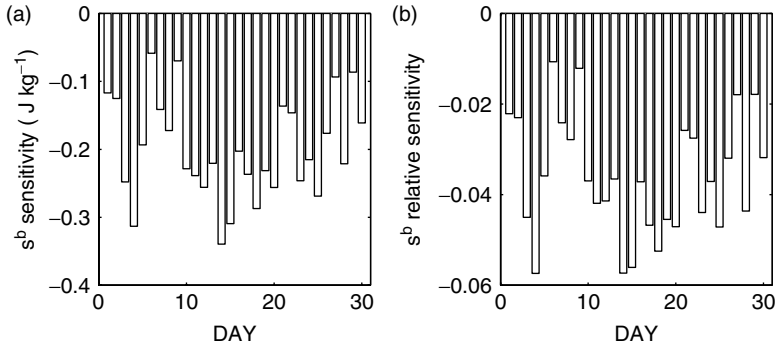

Figure 4. (a) Daily sensitivity of the 24 h forecast error to the 0000 UTC background-error covariance weighting coefficient s^b during August 2007. (b) shows the sensitivity normalized by the forecast error measure (%/%).

The explicit evaluation and the analysis of the full **B**-sensitivity matrix are not feasible in practical applications, however valuable information regarding the background-error correlations may be obtained by monitoring sensitivities to a specified error decorrelation length-scale. Additional practical difficulties in providing error covariance diagnostics are due to the fact that deficiencies in the representation of both background-error correlations and observational-error correlations may be present in operational data assimilation systems.

4.5. Preliminary results with NASA GEOS-5 DAS

Preliminary numerical experiments performed with the NASA GEOS-5 DAS (Rienecker *et al.*, 2008) are used to illustrate the practical ability of the adjoint-DAS approach to provide error covariance sensitivity information. GEOS-5 DAS consists of the GEOS-5 general circulation model comprising: finite-volume dynamics (Lin, 2004) and Goddard-developed physics; the adjoint of the finite-volume dynamics (Giering *et al.*, 2005) which accounts for simple vertical diffusion; the Grid-point Statistical Interpolation (GSI) analysis system (Wu *et al.*, 2002); and the adjoint of the GSI (Trémolet, 2007b). The computational overhead of calculating the sensitivities of interest consists of the integration of the adjoint of the GEOS-5 general circulation model to obtain the forecast sensitivity to initial conditions (8), evaluation of the observation sensitivity (5) by applying the adjoint-DAS operator, followed by the observation-space product with the vector of observed-minus-analysis. The necessary software tools have been developed at NASA Global Modeling and Assimilation Office (GMAO) and other major NWP centres for observation sensitivity and impact assessment and the additional capability of performing sensitivity to the specification of the error covariance weights is illustrated here.

Data assimilation and sensitivity experiments are performed at a horizontal resolution of $2.5^\circ \times 2^\circ$ with 72 hybrid levels in the vertical. To keep close to the theory discussed in previous sections, a single outer loop is used when running the forward GSI in GEOS-5 DAS; and consistently, the same applies when running the backward (adjoint) GSI. The model functional aspect (7) is specified as the 24 h average global forecast error between the model vertical grid levels 40 and 72 (from approximately 128 hPa down to the surface) in a total (dry) energy norm, with the verification state $\mathbf{x}_f^v$ provided by the DAS by performing 6 h analysis cycles. Statistics of the forecast sensitivity to multiplicative error covariance weighting coefficients (44) and (47) are collected for data valid at 0000 UTC during August 2007. For this period of experimentation, Daescu and Todling (2009) provided an adjoint-DAS assessment of the observation impact to the forecast-error reduction. Our new experiments illustrate the additional capability of performing sensitivity to the specification of the error covariance weights. GEOS-5 DAS assimilates observations from the conventional network: radiosondes, wind profilers, pilot balloon (PIBAL) winds, Aircraft to Satellite Data Relay (ASDAR) and Meteorological Data Collection and Reporting System (MDCARS) aircraft wind and temperature reports, NEXRAD radar winds, dropsonde winds, PAOB surface pressure, GMS and

Copyright © 2010 Royal Meteorological Society

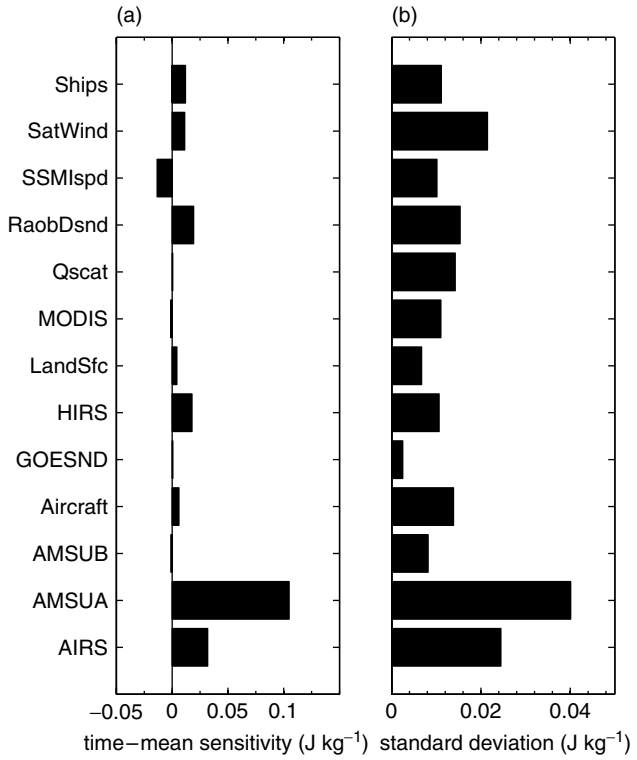

Figure 5. (a) Time-mean sensitivity of the 24 h forecast-error measure to the 0000 UTC observation-error covariance weighting coefficient s_i^o for various observing system components in August 2007. (b) shows the standard deviation of the time series of estimated sensitivities. The abbreviations for observation type along the vertical axis denote: *Ships*, ship and buoy temperatures, winds, specific humidities, and near-surface pressures; *SatWind*, cloud-drift winds; *SSMIspd*, Special Sensor Microwave Imager wind speeds; *RaobDsnd*, radiosonde and dropsonde temperatures, winds, specific humidities; *Qscat*, scatterometer winds; *MODIS*, Moderate-resolution Imaging Spectroradiometer clear-sky and water vapour winds; *LandSfc*, land observations of temperatures, winds, surface pressures, and specific humidities; *HIRS*, radiances from the High-resolution Infrared Radiation Sounder 3 from NOAA-16 and -17 satellites; *GOESND*, radiances from the Geostationary Operational Environmental Satellites; *Aircraft*, aircraft temperatures and winds; *AMSU-A*, radiances from the Advanced Microwave Sounding Unit-A on the NOAA-15, -16 and -18; *AMSU-B*, radiances from NOAA-15, -16 and -17, as well as NASA Aqua; *AIRS*, radiances from the Atmospheric Infrared Sounder on Aqua.

METEOSAT cloud-drift infrared (IR) and visible winds, MODIS clear-sky and water vapour winds, (GOES cloud-drift IR and water vapour cloud-top winds, surface land observations, SSM/I rain rates and wind speeds, Tropical Rainfall Measuring Mission Microwave Imager (TMI) rain rates, and QuickSCAT wind speeds and directions. Satellite radiances include: TIROS Operational Vertical Sounder (TOVS) level 1b AMSU-A from NOAA-15, -16 and -18, AMSU-B from NOAA-15, -16 and -17, HIRS-2 from NOAA-14, HIRS-3 from NOAA-16 and -17, Microwave Sounding Unit (MSU) from NOAA-14; Earth Observing System (EOS)/Aqua level 1b radiances AIRS and AMSU-A; GOES-10 and -12 sounder brightness temperatures; and Solar Backscattered Ultra-Violet (SBUV-2) (version 6) layer and total column ozone from NOAA-16. (Acronyms not explained here are given in the caption to Figure 5 below.)

Figure 4 displays the daily s^{b}-sensitivity (47) together with the associated relative sensitivities

$$\frac{\partial e(\overline{\mathbf{x}}^{\mathrm{a}})}{\partial s^{\mathrm{b}}}\frac{1}{e(\overline{\mathbf{x}}^{\mathrm{a}})}. \tag{67}$$

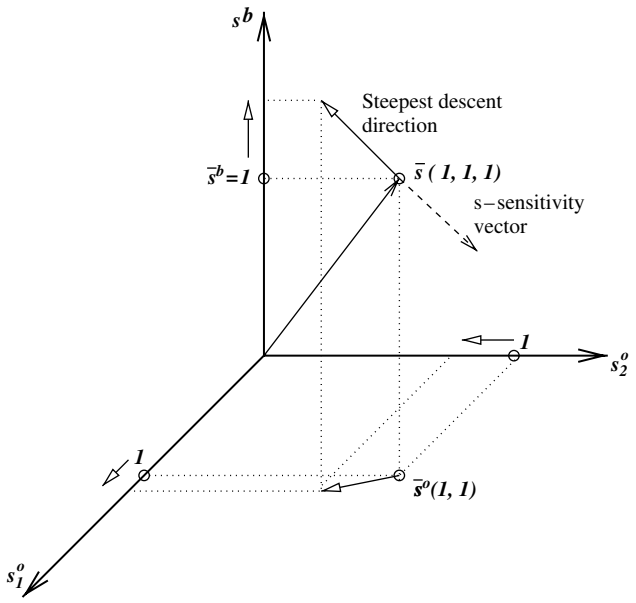

Figure 6. Illustration of the guidance provided by the forecast-error sensitivity to the DAS error covariance weight parameters. The sensitivity vector allows the identification of descent directions in the parameter space that may be used to achieve forecast-error reduction. Increasing the parameter values corresponds to the error covariance inflation in the DAS.

The s^{b}-sensitivity provides guidance on the proper weighting in the DAS between the information content of the background state and of the whole observing system and, in these experiments, the time-mean s^{b}-sensitivity was found to be $-0.2\,\mathrm{J\,kg^{-1}}$. Systematic negative values provide an indication that the background information is slightly over-weighted and that background-error covariance inflation is of potential benefit to the forecasts. The relative sensitivities (67) provide guidance on the percentage forecast impact as the result of variations in the s^{b} parameter from the nominal value of $\bar{s}^{\mathrm{b}} = 1$ and the time-mean relative sensitivity was estimated to be -0.037.

Figure 5 displays the time-mean sensitivities to observation-error covariance weights (44) and the standard deviation of the time series of sensitivity estimates for major observing system components. The sensitivity information describes the local behaviour of the forecast error aspect as a function of the error covariance parameters and provides valuable guidance to the parametric representation that is necessary to optimize the performance of error covariance tuning procedures. In Figure 5, the presence of positive sensitivity values for certain observing system components and of negative sensitivity values for other observing system components provides an indication that tuning of the observing system through a single scalar weight coefficient s^{o} ($I = 1$) is suboptimal and that improved results may be obtained by considering a multi-dimensional ($I > 1$) parametric representation (39). Figure 6 provides a geometrical illustration of the sensitivity guidance in a 3-dimensional parameter space $\mathbf{s} = (s^{\mathrm{b}}, s_1^{\mathrm{o}}, s_2^{\mathrm{o}})$ for a DAS configuration where at $\overline{\mathbf{s}} = (1, 1, 1)$ the derivatives values are such that $\partial e/\partial s^{\mathrm{b}} < 0$, $\partial e/\partial s_1^{\mathrm{o}} < 0$, and $\partial e/\partial s_2^{\mathrm{o}} > 0$: forecast error reduction may be achieved by individually varying a selected error covariance parameter while freezing all other parameters in the DAS or by simultaneously varying all error covariance parameters along a descent direction. For practical applications, the sensitivity information allows the identification of the steepest descent

Copyright © 2010 Royal Meteorological Society

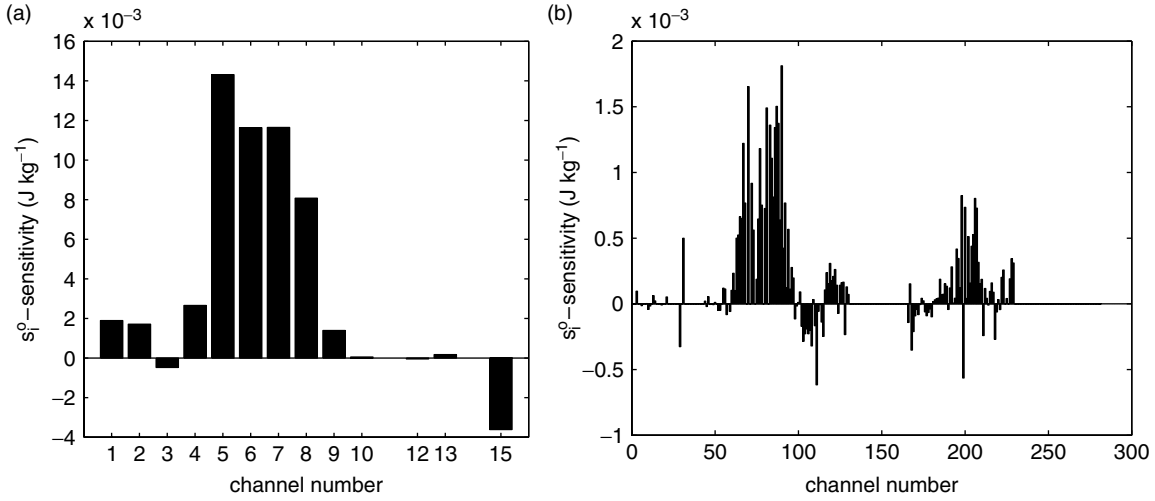

Figure 7. Time-mean sensitivity of the 24 h forecast-error measure to the 0000 UTC observation-error covariance weighting coefficient s_i^o per instrument channel for (a) NOAA-15 AMSU-A and (b) Aqua AIRS radiance data in August 2007.

direction (57) in the parameter space, and an additional iterative procedure is necessary to determine an optimal step length along this direction and to perform parameter tuning.

The observation-error covariance sensitivity analysis is particularly valuable for satellite data where accurate estimations of the observational errors (including measurement and representation errors) are difficult to provide. In these experiments, increased positive values were noticed for AMSU-A data, whereas increased negative values were noticed for SSM/I wind speeds. The preliminary aspect of the numerical results is emphasized and a systematic monitoring of sensitivities over an increased number of assimilation cycles is necessary to achieve statistical significance. The relevance of the adjoint sensitivity is closely determined by the specification of the forecast aspect, and objective measures are necessary to provide DAS diagnostics (Talagrand, 2003).

The forecast impact of tuning a satellite instrument may be improved if guidance is provided to distinguish between the instrument channels where increasing/decreasing the error covariance weight is of potential benefit to the forecasts. This adjoint-DAS ability is illustrated in Figure 7, where the time-mean forecast sensitivity to the observation-error covariance weighting coefficient s_i^o is displayed per instrument channel for data provided by the NOAA-15 AMSU-A and by the AIRS on NASA's Aqua satellite. Notice that not all channels from these instruments are used in the GEOS-5 DAS. For example, out of the set of 281 AIRS channels typically available for operations (Le Marshall *et al.*, 2006) only the cloud-cleared ones are actually used in the in GEOS-5 DAS and the sensitivity is shown for the 152 channels used in the assimilation cycles performed in these experiments. The large negative sensitivity of channel 15 of AMSU-A suggests that error covariance inflation for this channel could prove beneficial to the forecasts. However, one must keep in mind that this is a channel largely sensitive to the surface emissivity and cloud liquid water; in this case, the observation-error variance is intentionally set to be relatively large in comparison to the mid-troposphere and low-stratospheric channels 5 to 13. Similarly, at first glance, applying inflation to a number of AIRS channels could also result in improved 24 h forecasts. This is particularly so for some of the mostly water-vapour channels 162–214. Care must be exercised when evaluating the results for the window channels 117–130, where again observation errors are set intentionally large so they participate with little weight in the assimilation itself, and thus in determining the analysis and the verification state.

5. Conclusions

To date, the adjoint-DAS approach has been mainly considered in NWP as an effective tool to assess the value of observations in reducing the forecast errors and the forecast impact as a result of changes in the observing system. This study brings forward additional adjoint-DAS capabilities and applications based on the forecast sensitivity to the specification of error covariance parameters in the DAS. New theoretical aspects of error covariance sensitivity and forecast impact assessment are presented together with first illustrations of the adjoint-DAS ability to provide sensitivity information for DAS diagnostics and guidance to error-covariance parameter tuning procedures. Emphasis is placed on the intrinsic properties of the analyses derived from a minimization principle that are used to closely relate the error covariance sensitivity to the observation and background sensitivity. It is explained that the adjoint-DAS software tools developed at NWP centres for observation impact studies make feasible the evaluation of the forecast sensitivity to a large number of error covariance parameters. The adjoint-DAS observation impact assessment relies on information extracted from the innovations and observation sensitivity. In conjunction with the observation sensitivity, the observed-minus-analysis information provides an assessment of the weighting between the information content of various DAS input components, and allows the identification of the input components where improved estimates of the error statistics have a potentially large impact on the forecast error reduction. A proof-of-concept of gradient-based error-covariance parameter tuning was presented and the practical implementation and validation in a realistic DAS need to be further investigated. In practical applications, several simplifications are necessary to account for nonlinearities in the DAS, and the mathematical identities established

Copyright © 2010 Royal Meteorological Society

throughout this work should be regarded as approximate sensitivity relationships among various DAS components.

Modelling of the observation-, background-, and model-error correlations is an area of active research in NWP, and valuable information on the proper specification of the error correlation structure may be obtained by monitoring the forecast sensitivities to the error correlation parameters. The weak constraint 4D-Var allows the incorporation of the model error in the assimilation scheme and novel analysis tools are necessary to investigate the proper weighting of a time-distributed model error covariance. An extension of the adjoint-DAS sensitivity to account for model error parameters may be formulated and further research developments are needed in both theoretical and implementation aspects of this problem.

Acknowledgements

The work of D. N. Daescu was supported by the NASA Modeling, Analysis, and Prediction Program under award NNG06GC67G and by the National Science Foundation under award DMS-0914937. Resources supporting this work were provided by the NASA High-End Computing (HEC) Program through the NASA Center for Computational Sciences (NCCS) at Goddard Space Flight Center.

Appendix

In Daescu (2008), the forecast sensitivity to the specification of the error covariances in the DAS is expressed in column vector format using the vectorization operator vec and the Kronecker product (Magnus and Neudecker, 1999):

$$\nabla_{\mathrm{vec}(\mathbf{R})} e(\mathbf{x}^{\mathrm{a}}) = \{\mathbf{R}^{-1}\left[\mathbf{h}(\mathbf{x}^{\mathrm{a}}) - \mathbf{y}\right]\} \otimes \nabla_{\mathbf{y}} e(\mathbf{x}^{\mathrm{a}})\,, \tag{A1}$$

$$\nabla_{\mathrm{vec}(\mathbf{B})} e(\mathbf{x}^{\mathrm{a}}) = \left[\mathbf{B}^{-1}(\mathbf{x}^{\mathrm{a}} - \mathbf{x}^{\mathrm{b}})\right] \otimes \nabla_{\mathbf{x}^{\mathrm{b}}} e(\mathbf{x}^{\mathrm{a}})\,. \tag{A2}$$

The matrix format (14) and (16) to the error covariance sensitivity may be derived from (A1) and (A2) respectively, by noticing that, for any two column vectors **a** and **b**,

$$\mathbf{a} \otimes \mathbf{b} = \mathrm{vec}(\mathbf{b}\mathbf{a}^{\mathrm{T}})\,, \tag{A3}$$

and that for a scalar function e of matrix argument **X**,

$$\nabla_{\mathrm{vec}(\mathbf{X})} e = \mathrm{vec}\left(\frac{\partial e}{\partial \mathbf{X}}\right). \tag{A4}$$

References

Baker NL, Langland RH. 2009. Diagnostics for evaluating the impact of satellite observations. In *Data Assimilation for Atmospheric, Oceanic and Hydrologic Applications*. Park SK, Xu L. (eds.) JCSDA: Camp Springs, Maryland, USA. 177–196.

Baker NL, Daley R. 2000. Observation and background adjoint sensitivity in the adaptive observation-targeting problem. *Q. J. R. Meteorol. Soc.* **126**: 1431–1454.

Bannister RN. 2008a. A review of forecast-error covariance statistics in atmospheric variational data assimilation. I: Characteristics and measurements of forecast-error covariances. *Q. J. R. Meteorol. Soc.* **134**: 1951–1970.

Bannister RN. 2008b. A review of forecast-error covariance statistics in atmospheric variational data assimilation. II: Modelling the forecast-error covariance statistics. *Q. J. R. Meteorol. Soc.* **134**: 1971–1996.

Bergot T, Doerenbecher A. 2002. A study on the optimization of the deployment of targeted observations using adjoint-based methods. *Q. J. R. Meteorol. Soc.* **128**: 1689–1712.

Buehner M, Gauthier P, Liu Z. 2005. Evaluation of new estimates of background- and observation-error covariances for variational assimilation. *Q. J. R. Meteorol. Soc.* **131**: 3373–3383.

Cacuci DG. 2003. *Sensitivity and Uncertainty Analysis, Vol. 1: Theory*. Chapman & Hall/CRC Press: London and New York.

Cardinali C. 2009. Monitoring the observation impact on the short-range forecast. *Q. J. R. Meteorol. Soc.* **135**: 239–250.

Chapnik B, Desroziers G, Rabier F, Talagrand O. 2004. Properties and first applications of an error statistics tuning method in variational assimilation. *Q. J. R. Meteorol. Soc.* **130**: 2253–2275.

Chapnik B, Desroziers G, Rabier F, Talagrand O. 2006. Diagnosis and tuning of observational error in a quasi-operational data assimilation setting. *Q. J. R. Meteorol. Soc.* **132**: 543–565.

Cohn SE. 1997. An introduction to estimation theory. *J. Meteorol. Soc. Japan* **75**: 257–288.

Courtier P, Thépaut JN, Hollingsworth A. 1994. A strategy of operational implementation of 4D-Var using an incremental approach. *Q. J. R. Meteorol. Soc.* **120**: 1367–1388.

Daescu DN. 2008. On the sensitivity equations of four-dimensional variational (4D-Var) data assimilation. *Mon. Weather Rev.* **136**: 3050–3065.

Daescu DN. 2009. On the deterministic observation impact guidance: A geometrical perspective. *Mon. Weather Rev.* **137**: 3567–3574.

Daescu DN, Todling R. 2009. Adjoint estimation of the variation in model functional output due to the assimilation of data. *Mon. Weather Rev.* **137**: 1705–1716.

Daley R. 1991. *Atmospheric Data Analysis*. Cambridge University Press: Cambridge, UK.

Daley R, Barker E. 2001. NAVDAS: Formulation and diagnostics. *Mon. Weather Rev.* **129**: 869–883.

Dee DP. 1995. On-line estimation of error covariance parameters for atmospheric data assimilation. *Mon. Weather Rev.* **123**: 1128–1145.

Dee DP, Da Silva AM. 1999. Maximum-likelihood estimation of forecast and observation error covariance parameters. Part I: Methodology. *Mon. Weather Rev.* **127**: 1822–1834.

Desroziers G, Ivanov S. 2001. Diagnosis and adaptive tuning of observation-error parameters in a variational assimilation. *Q. J. R. Meteorol. Soc.* **127**: 1433–1452.

Desroziers G, Berre L, Chapnik B, Poli P. 2005. Diagnosis of observation, background, and analysis-error statistics in observation space. *Q. J. R. Meteorol. Soc.* **131**: 3385–3396.

Desroziers G, Berre L, Chabot V, Chapnik B. 2009. *Aposteriori* diagnostics in an ensemble of perturbed analyses. *Mon. Weather Rev.* **137**: 3420–3436.

Doerenbecher A, Bergot T. 2001. Sensitivity to observations applied to FASTEX cases. *Nonlinear Proc. Geophys.* **8**: 467–481.

Fourrié N, Doerenbecher A, Bergot T, Joly A. 2002. Adjoint sensitivity of the forecast to TOVS observations. *Q. J. R. Meteorol. Soc.* **128**: 2759–2777.

Frehlich R. 2006. Adaptive data assimilation including the effect of spatial variations in observation error. *Q. J. R. Meteorol. Soc.* **132**: 1225–1257.

Gaspari G, Cohn SE. 1999. Construction of correlation functions in two and three dimensions. *Q. J. R. Meteorol. Soc.* **125**: 723–757.

Gelaro R, Zhu Y, Errico RM. 2007. Examination of various-order adjoint-based approximations of observation impact. *Meteorol. Zeitschrift* **16**: 685–692.

Gelaro R, Zhu Y. 2009. Examination of observation impacts derived from observing system experiments (OSEs) and adjoint models. *Tellus* **61A**: 179–193.

Giering R, Kaminski T, Todling R, Errico RM, Gelaro R, Winslow N. 2005. Generating tangent linear and adjoint versions of NASA/GMAO's Fortran-90 global weather forecast model. In *Automatic Differentiation: Applications, Theory, and Implementations*. Vol. 50 of *Lecture Notes in Computational Science and Engineering*. Bücker HM, Corliss G, Hovland P, Naumann U, Norris B. (eds.) 275–284. Springer: New York.

Hamill TM, Snyder C. 2002. Using improved background-error covariances from an ensemble Kalman filter for adaptive observations. *Mon. Weather Rev.* **130**: 1552–1572.

Janjić T, Cohn SE. 2006. Treatment of observation error due to unresolved scales in atmospheric data assimilation. *Mon. Weather Rev.* **134**: 2900–2915.

Jazwinski AH. 1970. *Stochastic Processes and Filtering Theory*. Academic Press.

Joiner J, Brin E, Treadon R, Derber J, Van Delst P, Da Silva A, Le Marshall J, Poli P, Atlas R, Bungato D, Cruz C. 2007. Effects of data selection and error specification on the assimilation of AIRS data. *Q. J. R. Meteorol. Soc.* **133**: 181–196.

Kalnay E. 2002. *Atmospheric Modeling, Data Assimilation and Predictability*. Cambridge University Press: Cambridge, UK.

Copyright © 2010 Royal Meteorological Society

Langland RH. 2005. Observation impact during the North Atlantic TReC-2003. *Mon. Weather Rev.* **133**: 2297–2309.

Langland RH, Baker NL. 2004. Estimation of observation impact using the NRL atmospheric variational data assimilation adjoint system. *Tellus* **56A**: 189–201.

Le Dimet F-X, Ngodock H-E, Luong B, Verron J. 1997. Sensitivity analysis in variational data assimilation. *J. Meteorol. Soc. Japan* **75**: 245–255.

Le Marshall J, Jung J, Derber J, Chahine M, Treadon R, Lord SJ, Goldberg M, Wolf W, Liu HC, Joiner J, Woollen J, Todling R, van Delst P, Tahara Y. 2006. Improving global analysis and forecasting with AIRS. *Bull. Amer. Meteorol. Soc.* **87**: 891–894.

Li H, Kalnay E, Miyoshi T. 2009. Simultaneous estimation of covariance inflation and observation errors within an ensemble Kalman filter. *Q. J. R. Meteorol. Soc.* **135**: 523–533.

Lin SJ. 2004. A vertically Lagrangian finite-volume dynamical core for general circulation models. *Mon. Weather Rev.* **132**: 2293–2307.

Liu J, Kalnay E. 2008. Estimation of observation impact without adjoint model in an ensemble Kalman filter. *Q. J. R. Meteorol. Soc.* **134**: 1327–1335.

Lorenc AC. 2003. Modelling of error covariances by 4D-Var data assimilation. *Q. J. R. Meteorol. Soc.* **129**: 3167–3182.

Lorenz EN, Emanuel KA. 1998. Optimal sites for supplementary weather observations: Simulation with a small model. *J. Atmos. Sci.* **55**: 399–414.

Magnus JR, Neudecker H. 1999. *Matrix Differential Calculus with Applications in Statistics and Econometrics.* (Revised edition). John Wiley & Sons Ltd: New York and Chichester, UK.

Ménard R, Daley R. 1996. The application of the Kalman smoother theory to the estimation of the 4DVAR error statistics. *Tellus* **48A**: 221–237.

Rienecker MM, Suarez MJ, Todling R, Bacmeister J, Takacs L, Liu H-C, Gu W, Sienkiewicz M, Koster RD, Gelaro R, Stajner I, Nielsen JE. 2008. *The GEOS-5 Data Assimilation System – Documentation of versions 5.0.1, 5.1.0, and 5.2.0*. NASA/TM-2008-104606, Vol. 27, Tech. Rep. Series on Global Modeling and Assimilation. NASA Goddard Space Flight Center: Greenbelt, Maryland, USA.

Rosmond T, Xu L. 2006. Development of NAVDAS-AR: Non-linear formulation and outer loop tests. *Tellus* **58A**: 45–58.

Talagrand O. 1999. 'A posteriori verification of analysis and assimilation algorithms'. In *Proceedings of workshop on Diagnosis of Data Assimilation Systems*, 2–4 November 1998, 17–28. ECMWF: Reading, UK.

Talagrand O. 2003. 'Objective validation and evaluation of data assimilation' In *Proceedings of seminar on Recent Developments in Data Assimilation for Atmosphere and Ocean*, 8–12 September 2003, 287–299. ECMWF: Reading, UK.

Torn RD, Hakim GJ. 2008. Ensemble-based sensitivity analysis. *Mon. Weather Rev.* **136**: 663–677.

Trémolet Y. 2007a. Incremental 4D-Var convergence study. *Tellus* **59A**: 706–718.

Trémolet Y. 2007b. First-order and higher-order approximations of observation impact. *Meteorol. Zeitschrift* **16**: 693–694.

Trémolet Y. 2008. Computation of observation sensitivity and observation impact in incremental variational data assimilation. *Tellus* **60A**: 964–978.

Wu W, Purser RJ, Parrish DF. 2002. Three-dimensional variational analysis with spacially inhomogeneous covariances. *Mon. Weather Rev.* **130**: 2905–2916.

Zhu Y, Gelaro R. 2008. Observation sensitivity calculations using the adjoint of the Gridpoint Statistical Interpolation (GSI) analysis system. *Mon. Weather Rev.* **136**: 335–351.

Copyright © 2010 Royal Meteorological Society